

Quantitative Tool Characterization of a 193 nm Scatterfield Microscope

Martin Y. Sohn*, Bryan M. Barnes, Hui Zhou and Richard M. Silver

National Institute of Standards and Technology, 100 Bureau Drive, Gaithersburg, MD, 20899-8212

ABSTRACT

An investigation of an optical microscope tool characterization was presented for the quantitative measurements of deep sub-wavelength features using Fourier plane normalization method. The NIST 193 nm scatterfield microscope operating with an ArF Excimer laser, which has a capability of articulating the angular incident beam at the sample plane using an aperture scanning at the conjugate back focal plane (CBFP), was characterized through the illumination and collection optical paths. Each incident cone beam at the sample plane can be approximated as a plane wave as in Köhler configuration, simplifying the analysis of the scattered light induced by the discrete illumination beam at the sample plane. Under this approximation, the illumination and entire tool function sets were measured at the sample and imaging CCD planes, respectively, producing the collection tool function set numerically. The two sets of optical tool functions will be used to normalize scattering simulations in the Fourier space domain of the CCD image in the collection path. We investigated some aspects of the beam distributions of the illumination beam at the sample plane with respect to the change of the optical components and report the illumination and collection tool function distributions that were obtained by angular scanning of an aperture at conjugate back focal plane.

Keywords: Quantitative microscope characterization, uncertainty, scatterfield microscopy, optical metrology, illumination tool function, collection tool function.

1. INTRODUCTION

Quantitative optical measurements of deep-subwavelength critical dimensions (CDs) with imaging microscopy for semiconductor manufacturing require rigorous comparisons between experimental data and simulations. Recently, NIST has made quantitative measurements of a Si step edge and of a periodic grating using a microscope of $\lambda = 450$ nm [1]. These measurements were performed with focus-resolved imaging to obtain information about the three-dimensional scattered intensities, and simulations were likewise performed using parametric models of the sample geometries that yielded images at several positions below and above the substrate. To facilitate optimal simulation-to-experiment matching, data were normalized to better reflect the deviations of the actual microscope from the idealized microscope. "Tool functions" for the illumination and collection optical paths were determined to correct for intensity inhomogeneities for the incident light and for losses in the collection path for the scattered light. The illumination corrections were applied to the experimental data as a function of incident angle, while the collection path corrections were applied to the Fourier components of the scattered light.

Tool functions, therefore, represent optical and mechanical errors in the optical paths and are essential for the Fourier plane normalization method. These tool functions can be described with respect to the incident and scattered angles at the sample plane. Scatterfield microscopy, an optical alternative technique for nanoscale metrology that overcomes conventional diffraction limits defined by wavelength and numerical aperture [2, 3], is a useful method enabling angle-resolved illumination that, when paired with a 0th-order sample, offers angle-resolved reflection that enables angular tool characterization throughout the optical path. The National Institute of Standards and Technology (NIST) 193 nm scatterfield microscope can likewise engineer the angular illumination and collection of beam propagation with respect to the incident and scattered angle at the sample plane. Here, this is used to characterize the effects of error information through the optical path by scanning an aperture over a large conjugate back focal plane (CBFP), resulting the illumination and collection tool function distributions [4, 5].

In this paper we present a simulation and a preliminary experimental investigation of the tool characterization with respect to the angle at the sample plane and report the experimental distribution of the illumination and collection tool functions obtained from the NIST 193 nm scatterfield microscope platform. This study is a key first step towards

*martin.sohn@nist.gov

quantitative measurements of critical dimensions using an imaging $\lambda = 193$ nm microscope, although further experiments and sensor calibrations are required as part of a comprehensive analysis that is currently ongoing.

2. INFLUENCE OF TOOL FUNCTIONS

The NIST $\lambda = 193$ nm microscope is a reflection optical imaging microscope that can be thought of as having two optical paths, as shown in Figure 1: First, the illumination path, in which a beam from the source (S) illuminates the sample plane (SP) at an incident angle through the conjugate back focal plane (CBFP) and the back focal plane (BFP) of the objective lens (OL). Second, the collection path, in which the scattered beam from the sample plane (SP) arrives at the image plane (IP) through the back focal plane (BFP). Due to a Köhler configuration in the illumination path, a point at the CBFP generates an incident plane wave at the SP through the BFP, and the reflected and scattered waves from the SP generate a Fourier component distribution at the BFP composing an image at the IP. The angular beam propagation over the illumination and collection optical paths, respectively, results in intensity distributions with respect to the incident angle at the sample plane. These two angular intensity distributions contain beam propagation errors induced by the components of the optical paths and are called the illumination and collection tool functions. These angle resolved tool functions can be used in the Fourier domain normalization method for image profile reconstruction.

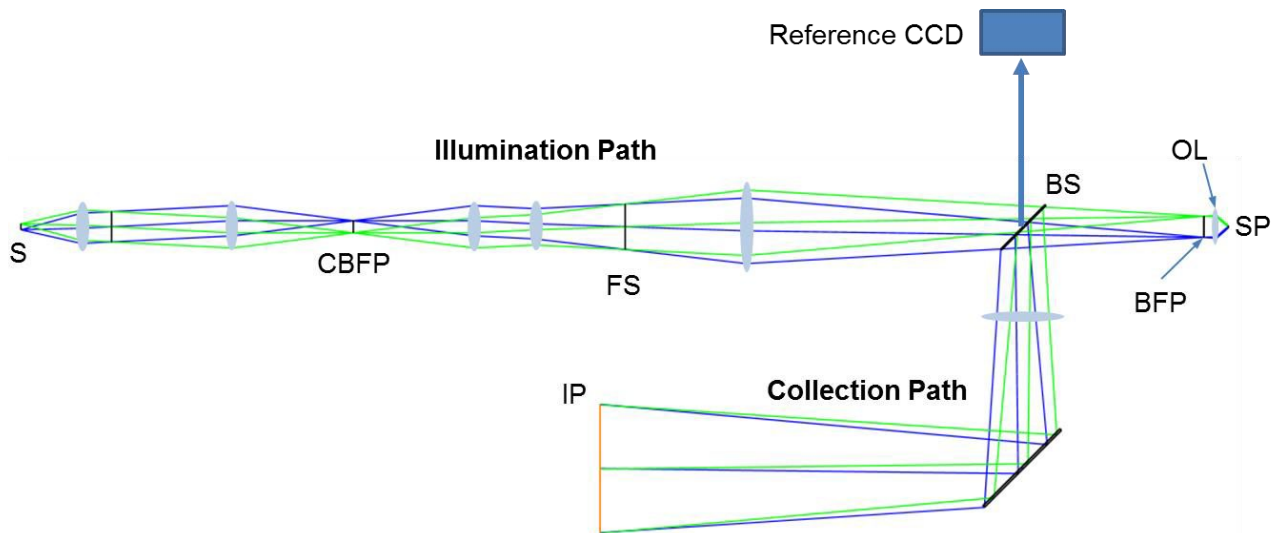


Fig. 1. Schematic of the microscope optical path; S source, CBFP: conjugate back focal plane, FS: field stop, BS: beamsplitter, OL: objective lens, BFP: back focal plane, SP: sample plane, IP: image plane. A point at CBFP generates an incident plane wave at SP by Kohler configuration in the illumination path and the scattered waves from SP generate Fourier component distribution at BFP composing an image at IP, enabling the illumination and collection tool function in angle term, respectively. The reference CCD is used to normalize the laser intensity for both tool functions.

The two tool functions are described in Eq. (1) as the factors operated to the illumination field E_i at the sample plane in Figure 2, which shows the image formation through the Fourier components by the light field scattering.

$$E_s = \left(TF_c^{m=0} \cdot M_s^{m=0} + TF_c^{m=1} \cdot M_s^{m=1} \right) \cdot TF_i \cdot E_0 \quad (1)$$

The illumination plane wave field E_i , which is the source field E_0 modified by the illumination tool function TF_i , becomes the angularly scattered fields E_s with scattering factors M_s indexed by the scattering order m . The scattering factor represents the target geometry determining the scattering direction, phase, and amplitude. In the collection path

the Fourier components at the pupil plane contribute additively at the image plane to image formation, with each Fourier component modified by the collection tool function TF_c . These tool functions contain the attenuation and the optical deviations induced by the optical paths. If these tool functions are known or approximated in terms of the illumination angle, the Fourier components can be normalized by the tool functions at the pupil plane, allowing reconstruction of the corrected image at the image plane.

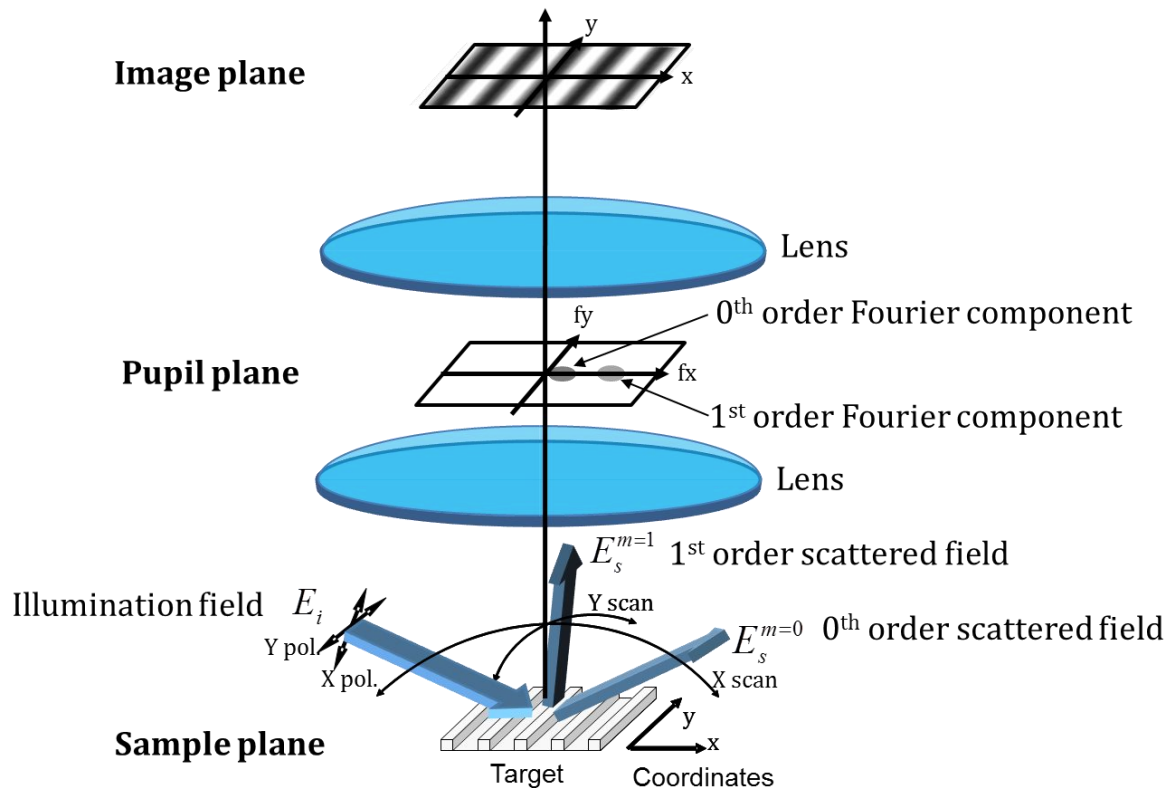


Fig. 2. Schematic of the image formation by light field scattering. The illumination plane wave field E_i , which is the source field E_0 modified by the illumination tool function TF_i , becomes the angularly scattered fields E_s with scattering factors M_s , indexed by the scattering order m . The Fourier components at the pupil plane contribute additively to image formation at the image plane with the collection tool function.

The illumination tool function is measured underneath the sample plane by a detector while an aperture is positioned in and moved within the CBF, and the collection tool function is indirectly obtained from both the entire tool function that is measured at the image plane and the illumination tool function. Each of these tool functions are relative to the polarization as defined in Figure 2. The two tool functions affect the Fourier components at the pupil plane by which the simulated image profiles at the image plane are corrected.

Since the tool function distributions are referenced to the illumination angle at the sample plane, the illumination tool functions are primarily investigated and Figure 3 shows examples of the illumination tool errors that are simulated using a geometrical ray tracing method, showing that the alignment errors change the illumination distribution with respect to the illumination angle. The left column of Fig. 3 shows the illumination distributions for source displacement, lens lateral and axial displacements, and lens tilt, and in the right column are the differential graphs with respect to the reference illumination distributions. In the right column, the central dip is caused by occlusion inherent to the catadioptric objective lens. The displacement amounts were less than about 1% of each component. It is noted that the edge sides are affected by the components errors except for the case of axial displacement, meaning that larger angles in the Fourier component distribution are more dominantly affected by the tool functions.

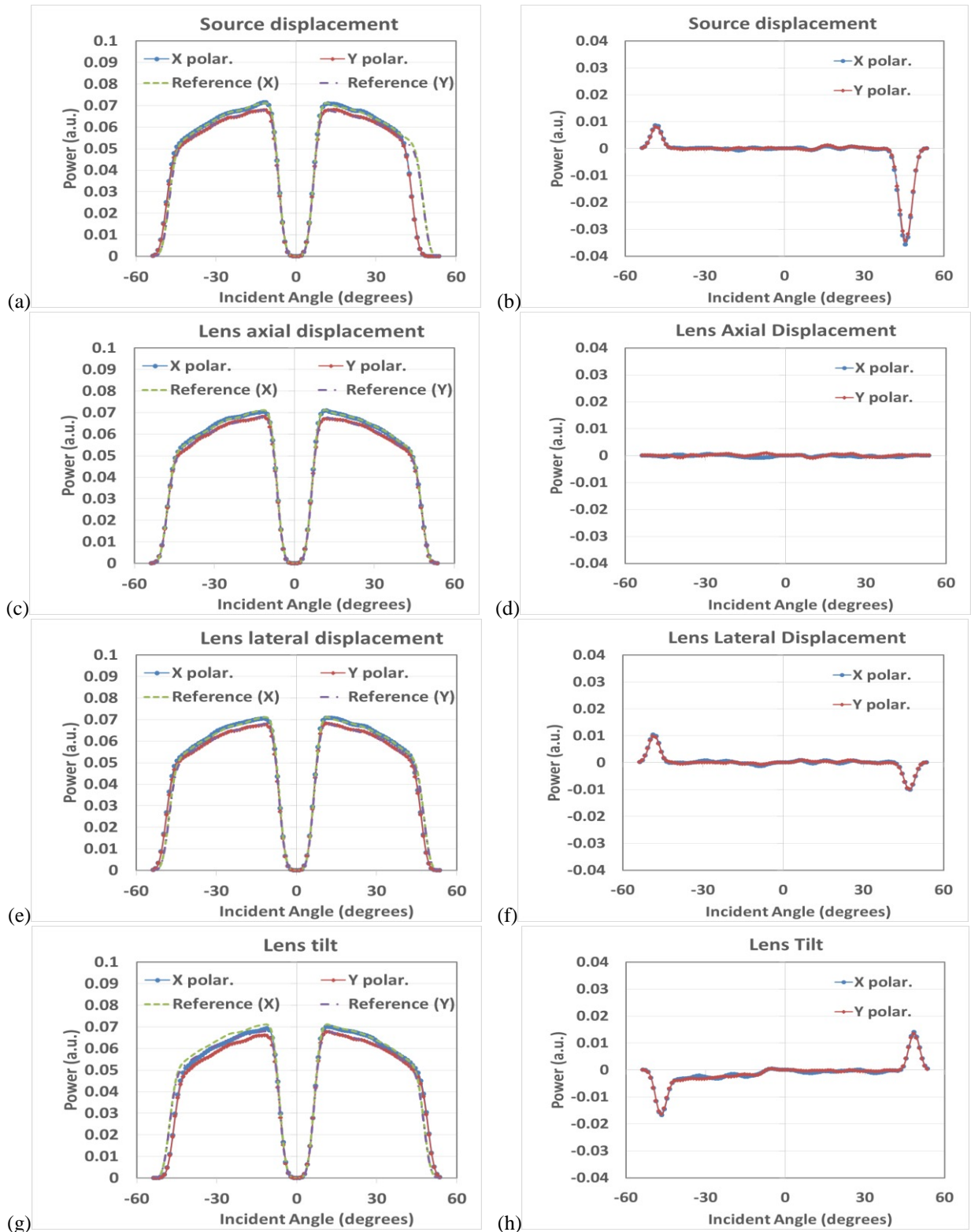
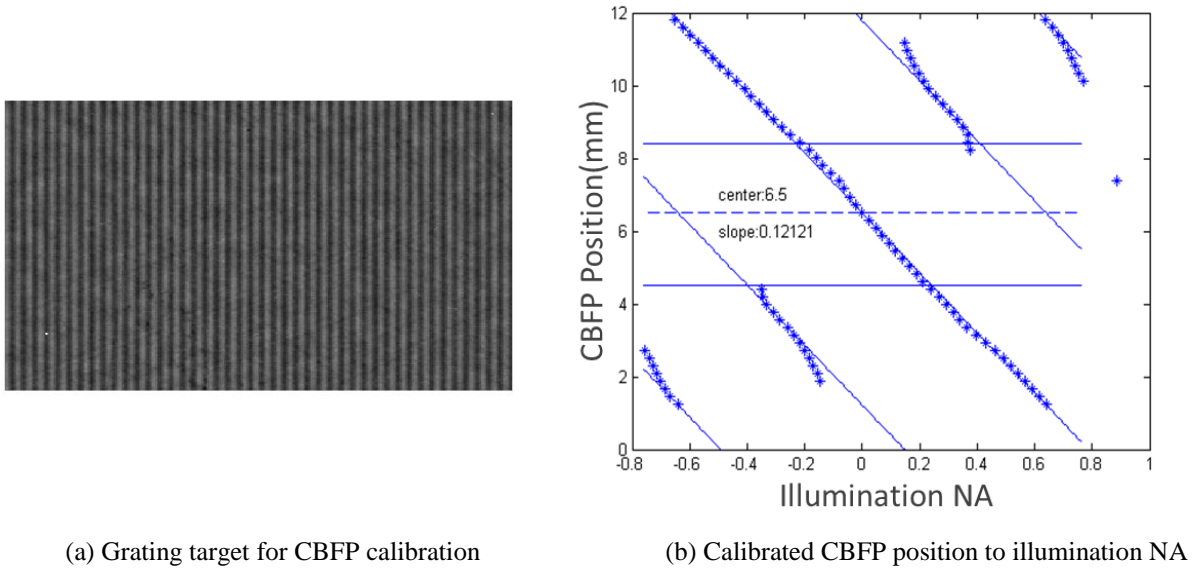


Fig. 3. Angular illumination distributions for optical component errors. The left and right graphs show raw and differential data, and (a), (b) represent source displacement of 0.1 mm, (c), (d) lens lateral displacement of 0.1 mm, (e), (f) lens axial displacement of 0.1mm, and (g), (h) lens tilt of 0.1° .

3. EXPERIMENTS

The NIST 193 nm Microscope has a telecentric CBFP with a 12 mm diameter, a catadioptric objective lens of NA = 0.12 to 0.74, and a high resolution CCD camera with a 14 μm pixel pitch. The tool characterization procedure for quantitative measurement begins with the measurement of the illumination tool function distribution. As the illumination is provided using an Excimer laser at the deep ultraviolet wavelength, an additional correction is also made to account for laser energy fluctuations inherent to these lasers. For this intensity correction, a second CCD camera was located at an alternative optical path from a beam splitter as shown in Fig. 1. In addition, the relationship between CBFP position and illumination angle must be calibrated.



(a) Grating target for CBFP calibration (b) Calibrated CBFP position to illumination NA

Fig. 4. Calibration of conjugate back focal plane (CBFP). (a) Fourier-filtered $\lambda=193$ nm microscope image of a calibrated diffraction grating of 100 nm lines with 300 nm period, and (b) Measured data to calibrate the illumination angle with respect to CBFP position. Here, CBFP position is the independent variable and the axes are rotated for illustration.

The relationship between CBFP position and angle was calibrated using the well-known grating diffraction theory described as Eq. (2), where d , θ_i , θ_m , m , λ are line pitch, incident and diffracted angles, diffraction order, and wavelength. Figure 4 (a) shows a Fourier-filtered image of a nominally 100 nm line grating with a 300 nm period that has been measured by SEM and scatterfield microscopy.[Add Ref] Knowing the grating pitch and varying the position of CBFP, the diffracted beam positions are discretely measured at the pupil plane. Figure 4 (b) shows the relationship between the center of a given diffracted beam image in the pupil plane and its corresponding equivalent illumination numerical aperture, $INA = \sin \theta$ as calculated according to

$$d(\sin \theta_i - \sin \theta_m) = m\lambda \quad (2)$$

The aperture diameter for angular scanning was 1 mm in diameter and the scan step was 0.2 mm.

The illumination and collection tool function distributions were obtained as shown in Fig. 5 with respect to the polarization direction. The illumination tool function distributions of (a), (c) represent the illumination errors induced from the components showing difference for the illumination polarizations. For the entire tool function measurement a blank silicon wafer was used, after accounting for the theoretical dependence of the reflectivity of Si upon the incident angle and polarization. These tool function distributions are to be used to correct the simulated images through the Fourier domain normalization at the pupil plane in the collection path.

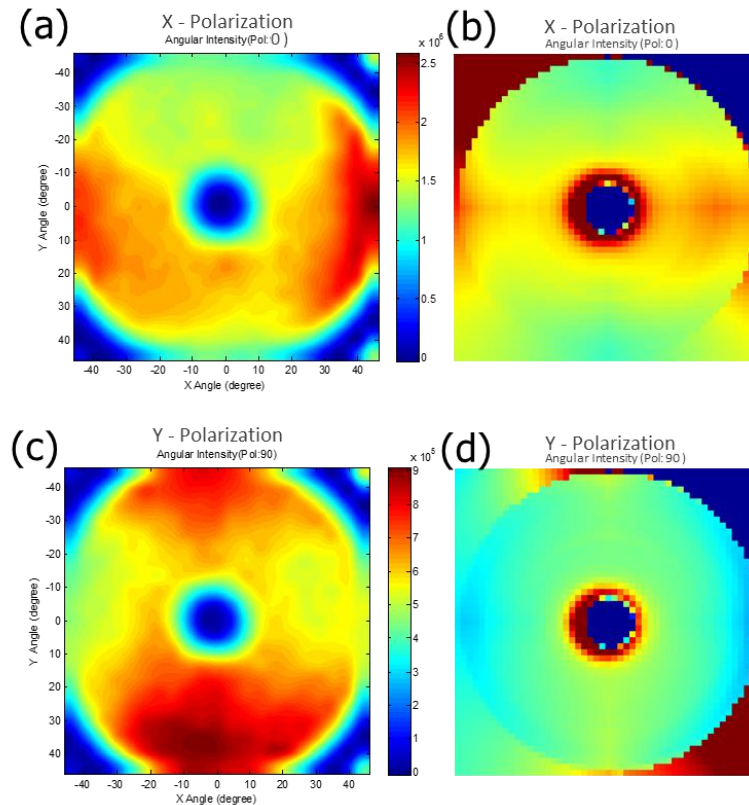


Fig. 5. Measured tool functions; (a), (c) show the illumination tool functions and (b), (d) the collection tool functions.

4. SUMMARY

The NIST 193 nm scatterfield microscope was characterized by measuring tool functions for correcting simulation data integral to the Fourier domain normalization method to improve data fitting between experiment and simulations with parametrized geometries. Several illumination intensity distributions were investigated using a geometrical ray tracing method, and preliminary experiments were obtained measuring the illumination tool function underneath the sample plane. The collection tool function was also obtained indirectly from the entire and illumination tool functions. The influence of alignment errors upon tool functions are measurable and must be minimized as a first step toward achieving quantitative measurements using Fourier domain normalization at $\lambda = 193$ nm.

References

- [1] J. Qin, R. M. Silver, B. M. Barnes, H. Zhou, and F. Goasmat, "Fourier domain optical tool normalization for quantitative parametric image reconstruction," *Appl. Opt.* 52 (26), 6512 – 6522 (2013).
- [2] R. M. Silver, B. M. Barnes, A. Heckert, R. Attota, R. Dixson and J. Jun, "Angle resolved optical metrology," *Proc. SPIE* 6518, 69221M (2008).
- [3] R. M. Silver, B. M. Barnes, R. Attota, J. Jun, M. Stocker, E. Marx, and H. J. Patrick, "Scatterfield microscopy for extending the limits of image-based optical metrology," *App. Optic.* 46 (20), 4248 – 4255 (2007).
- [4] Y. J. Sohn, Richard M. Silver, "Kohler illumination analysis for high-resolution optical metrology using 193 nm light," *Proc. SPIE* 6518, 65184V (2007).
- [5] Y. J. Sohn, R. Quintanilha, Lowell Howard, and R. M. Silver, "Analysis of Kohler illumination for 193 nm scatterfield microscope," *Proc. SPIE* 7272, 72723T (2009).